X International Conference on Textile Composites and Inflatable Structures
STRUCTURAL MEMBRANES 2021
K.-U.Bletzinger, E. Oñate, R. Wüchner and C. Lázaro (Eds)

CONSISTENT ALGORITHM FOR TENSEGRITY FROM FORM-FINDING TO FOLDING AND DEPLOYMENT SIMULAITON WITH COMMON SCHEME

CHO KYI SOE*, S. YAMASHITA†, E. KARASNIQI*, K. IJIMA* AND H. OBIYA*

* Department of Science and Engineering
Saga University, Japan
1 Honjo, Saga, 840-8502, Japan
E-mail : chokyisoe@gmail.com

† Miyaji Engineering Co., Ltd.
Ichihara Shi, Japan
103-0014, Japan
Email : yamashita.shuhei@miyaji-eng.co.jp

Key words: Tensegrity Simulation, Consistent Algorithm, Common Scheme.

Summary. In this study, we developed an algorithm which can consistently conduct from form-finding process using virtual elements to static/dynamic simulation process of folding and deployment with hyper-elastic elements. This algorithm provides both processes by common scheme of the tangent stiffness method which is quite effective in the geometrical nonlinear analysis due to its strict rigid body displacement of elements. The algorithm has more rationality than in case of using the force density method in the form-finding process.

1 INTRODUCTION

In recent decades, tensegrity has gained its popularity due to its mysterious geometric morphology and significant characteristics. The unique behaviour of tensegrity structures has been investigated in different ways for years, concerning form-finding [1], folding/deployment [2] and dynamic applications [3]. For example, Kan et al. [4] conducted the deployment analysis and studied the nonlinear dynamic behavior of clustered tensegrity structure using a positional FEM formulation. Pinaud et al. [5] modeled a small-scaled tensegrity boom and investigated the asymmetrical configurations under the deployment by controlling the tendon. The ordinary nonlinear differential equations were applied in the literatures of Sultan and Skelton to develop a dynamic model during the deployment process of tensegrity structure [6]. Masic and Skelton [7] conducted the dynamic control performance and optimized the pre-stress of a tensegrity structure by using the linearized dynamic model. With an experimental study, Chan et al. [8] performed an active vibration control of a triple-layered tensegrity structure in which the active damping is controlled by the force and acceleration feedback. Later, Ali and Smith [3] proposed vibration control for a full-scale active tensegrity structure by modifying the self-stress which influences the dynamic behavior. In this study, tensegrity structure will undergo a series of geometrical nonlinear analyses implemented by the consistent algorithm, simulating the proposed model with a stable self-equilibrium condition.

2 CONSISTENT ALGORITHM

The proposed consistent algorithm includes four main parts. The first part is form-finding process using the virtual elements of measure potential. After the equilibrium shape is determined, each member is substituted by the real elements such as aluminum for strut and rubber material for the cable. In the second part, the self-equilibrated tensegrity having the real stiffness undergoes the free vibration simulation. The Eigen value analysis is carried out and its displacement modes are examined to calculate the damping coefficients. The third part is folding process in which the proposed model is perfectly folded by the compulsory displacement. The folded tensegrity is taken back to its original configuration by the deployment process in the final part. This is accompanied by the dynamic simulation in which the tensegrity structure makes its full-scale deployment and the reduction of kinematic energy in its oscillatory mechanism is achieved by giving the appropriate amount of damping.

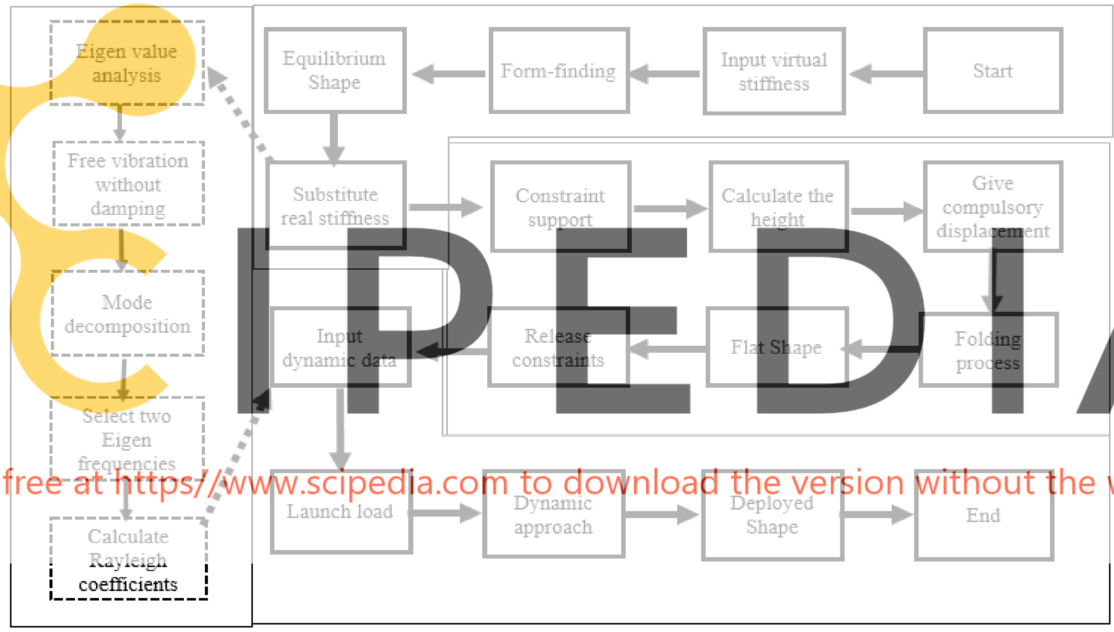

Figure 1: Flow of consistent algorithm

3 FORM-FINDING ANALYSIS

3.1 Measure potential and element force equation

The shape formation is mainly governed by the element behavior and the member forces bearing the stiffness. In this study, the geometrical nonlinear problems are solved by tangent stiffness method (TSM) where $\boldsymbol{B}$ is the nodal force vector, $\boldsymbol{K_0}$ is the element stiffness, $\boldsymbol{K_G}$ is the tangent geometrical stiffness and $\boldsymbol{d}$ is the nodal displacement vector.

$$\delta \boldsymbol{B} = (\boldsymbol{K_G} + \boldsymbol{K_0})\delta \boldsymbol{d} \tag{1}$$

In the form-finding process by TSM, the element behavior can be achieved by defining the measure potentials which are virtual functions having the parameters of element measurement.

In this study, the measure potential P is described by power function as follow.

$$P = c(l - l_0)^{n+1} \tag{2}$$

The element force equation can be derived from the differentiation of measure potential.

$$N = (n+1)c(l - l_0)^n = C(l - l_0)^n \tag{3}$$

in which N is axial force, C is the coefficient of stiffness, n is the multiplier, l is the current length and l_0 is the non-stressed length of elements. Note that defining the element potential can be assumed as virtual element stiffness that does not relate to the material's stiffness. Therefore, the assignment of each coefficient can freely be user-defined as shown in table 1.

Table 1: Assignment of designated values for each coefficient of element force equation

Element force equation	$N = C(l - l_0)^n$	
Related coefficients	For stiffer elements (strut)	For softer elements (cable)
C	EA/l_0 ($EA = 2 \times 10^{11}$)	0.8
n	1	3
l_0	7.0	0.0

Here, the strut of proposed tensegrity is defined by the linear function of n=1, making it similar to the truss behavior with relatively high value of stiffness coefficient. On the other hand, the multiplier n of cable member is assigned to have a multiple number with very low stiffness. Therefore, the tangent stiffness equation can be prepared as follow.

$$\delta \begin{bmatrix} \boldsymbol{B}_i \\ \boldsymbol{B}_j \end{bmatrix} = \boldsymbol{K}_G + \boldsymbol{K}_0 = \left\{ \frac{N}{l} \begin{bmatrix} \boldsymbol{e} - \boldsymbol{JJ}^T & \boldsymbol{JJ}^T - \boldsymbol{e} \\ \boldsymbol{JJ}^T - \boldsymbol{e} & \boldsymbol{e} - \boldsymbol{JJ}^T \end{bmatrix} + nC(l - l_0)^n \begin{bmatrix} \boldsymbol{JJ}^T & -\boldsymbol{JJ}^T \\ -\boldsymbol{JJ}^T & \boldsymbol{JJ}^T \end{bmatrix} \right\} \delta \begin{bmatrix} \boldsymbol{d}_i \\ \boldsymbol{d}_j \end{bmatrix} \tag{4}$$

The connectivity of members and the designated support condition are selected appropriately and the rotational conversion of members is calculated properly so that the obtained equilibrium solution figure 2(b) will be almost the same as the primary unbalanced form figure 2(a). The resulted tensegrity is three-dimensional configuration in self-equilibrated and stable condition in which the brown color refers to the compression force carried by the strut and the red color illustrates the tensile force suffered in the cables.

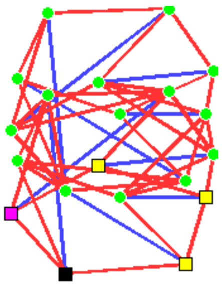

(a) Primary unbalanced form

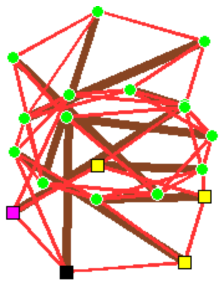

(b) Equilibrium form

Figure 2: Finding equilibrium solution by shape analysis

However, the shape formation derived by the form-finding keeps its equilibrium state by the tension or compression element forces by the virtual stiffness. Therefore, by using the Newton-Raphson method, the actual non-stressed length of each member is re-calculated depending on the amount of element edge forces which governs the shape formation of equilibrium solution. After the derivation of actual non-stressed length, each and every member of the whole tensegrity is substituted by the real material stiffness.

Since one of the unique characteristics of tensegrity is "being lightweight", the main supporting stiffer elements (strut) is designed to have material stiffness of aluminum with Young's modulus of 68 GPa and cross-sectional area of 0.01 m^2. Moreover, the tensegrity itself has a strong nonlinearity and can deform in a large scale compared to other structures, the material to be applied in cable members should be in high compatibility with large deformation process. This is achieved by analyzing the mechanical behavior of rubber-like hyper-elastic elements that can response elastically even under the large loading condition. In this study, the Ogden model is used and the nominal stress F from the derivation of strain energy function is

$$F = \sum_{i=1}^{K} \mu_i \left(\lambda^{\alpha_i - 1} - \lambda^{-1-\frac{\alpha_i}{2}}\right) \tag{5}$$

where, λ is the principal stretch, K is the serial number (here, we will use K=3) and μ_i, α_i are shear modulus and material property value respectively. A simple uniaxial test of rubber material is conducted to identify these physical properties from the obtained stress and the values are as below.

$$\alpha_1 = 0.88, \alpha_2 = 5.31, \alpha_3 = -1.01 \tag{6}$$

$$\mu_1 = 7.15 \times 10^{-1}, \mu_2 = 2.05 \times 10^{-2}, \mu_3 = -9.10 \times 10^{-2} [N/mm^2] \tag{7}$$

The Ogden model shows the characteristic of stiffness hardening both in tension and compression zones. However, when we assume the compression-free elements such as rubber cord, softening occurs in the compression side. Therefore, the square root function is introduced to realize the relaxation process.

$$F(\lambda) = -\sqrt{a\lambda + b} - c \tag{8}$$

The coefficients *a, b* and *c* in equation (8) are smoothly connected to the Ogden model by Lagrange interpolation. In the case of one-dimensional cable element connecting two nodes, the element force equation which defines the element's own behavior can be expressed as:

$$N = F(\lambda) A_0 \tag{9}$$

where, N is axial force and A_0 is the primary cross-sectional area of element and the corresponding tangent stiffness equation can be prepared as below.

$$\delta \begin{bmatrix} \boldsymbol{B}_i \\ \boldsymbol{B}_j \end{bmatrix} = \boldsymbol{K_G} + \boldsymbol{K_0} = \left\{ \frac{N}{l} \begin{bmatrix} \boldsymbol{e} - \boldsymbol{JJ}^T & \boldsymbol{JJ}^T - \boldsymbol{e} \\ \boldsymbol{JJ}^T - \boldsymbol{e} & \boldsymbol{e} - \boldsymbol{JJ}^T \end{bmatrix} + \frac{\partial F}{\partial \lambda} \cdot \frac{A_0}{l_0} \begin{bmatrix} \boldsymbol{JJ}^T & -\boldsymbol{JJ}^T \\ -\boldsymbol{JJ}^T & \boldsymbol{JJ}^T \end{bmatrix} \right\} \delta \begin{bmatrix} \boldsymbol{d}_i \\ \boldsymbol{d}_j \end{bmatrix} \tag{10}$$

In this way, in the common scheme of tangent stiffness method, the user can define any type of element force equation depending on the material and the mechanical properties while the rigid body displacement is strictly maintained in the geometrical stiffness matrix.

4 SIMULATION OF DYNAMIC ANALYSIS

In this section, the obtained equilibrium tensegrity will be simulated by the free oscillatory mechanism with no damping effect. In general, the equation of motion can be expressed as:

$$\boldsymbol{M}\ddot{u} + \boldsymbol{C}\dot{u} + \boldsymbol{K}\Delta u = \boldsymbol{B} \tag{11}$$

where, $\boldsymbol{M}$ is mass matrix, $\boldsymbol{C}$ is damping matrix, $\boldsymbol{K}$ is stiffness matrix, $\boldsymbol{B}$ is external force, $\ddot{u}$ is acceleration, $\dot{u}$ is velocity and Δu is displacement. In the case of free vibration without damping, only the mass matrix and stiffness matrix are considered in calculation since the load term and the damping matrix will become zero. Therefore, free vibrational movement of the structure can be fully observed and decomposed into mode displacement by means of eigenvalue analysis.

4.1 Mode decomposition

When a structure is in oscillation under damping, the damping matrix is needed to be considered in the equation of motion. However, the amount of damping is quite difficult to measure in practical compared to that of mass or stiffness of the structure. On the other hand, it is possible to characterize the damping effect by applying the appropriate formularization in the dynamic theory. Damping matrix in the dynamic equation can be expressed by two terms, named Rayleigh damping coefficients. These can be determined by the orthogonality of damping matrix for a mode shape. With the appropriate treatment of Rayleigh damping coefficients, the result of dynamic analysis of multi-degree of freedom system can be taken as the same as the experimental data. Rayleigh coefficients can be computed from damping matrix $\boldsymbol{C}$ of following equation.

$$\boldsymbol{C} = \alpha\boldsymbol{M} + \beta\boldsymbol{K} \tag{12}$$

where, α is proportional to mass matrix $\boldsymbol{M}$ and β is proportional to stiffness matrix $\boldsymbol{K}$.

$$\alpha = \frac{2\omega_i\omega_j.(\zeta_i.\omega_j - \zeta_j.\omega_i)}{{\omega_j}^2 - {\omega_i}^2} \tag{13}$$

$$\beta = \frac{2.(\zeta_j.\omega_j - \zeta_i.\omega_i)}{{\omega_j}^2 - {\omega_i}^2} \tag{14}$$

If two damping ratio are assumed to have the same value, then α and β can be simplified as

$$\alpha = \frac{2\omega_i\omega_j\zeta}{\omega_i + \omega_j} \tag{15}$$

$$\beta = \frac{2\zeta}{\omega_i + \omega_j} \tag{16}$$

In order to calculate Rayleigh coefficients, the required Eigen frequencies can be obtained by analyzing mode decomposition of the structural displacement. Eigen values for each mode can be derived by the Eigen value analysis form free vibration system before determining the damping effect. The equilibrium model shown in figure 2(b) undergo the free vibration for given time lap of 3 seconds and its total energy is conserved until around 0.7 second as in figure 3. Then, the mode decomposition will be examined by the Eigen value analysis. In the tensegrity system, one free node has 3-degree-of-freedom, and the proposed model has total 20 nodes. However, the base nodes of model are given by 8 constraints so that total 52-degree-of-freedom will be obtained in the free vibration mechanism. Therefore, total 52 eigenvalues and corresponding eigenvectors are obtained by Jacobi method as in table 2. Investigating the mode displacement pattern of figure 4, the 3rd and 20th modes are selected as two Eigen frequencies to calculate the Rayleigh coefficients since these two modes demonstrate the relatively significant displacement among the total mode patterns. Meanwhile, the damping ratio is assigned to have the same value of 0.2 and the corresponding α and β can be calculated by equation (15) and (16).

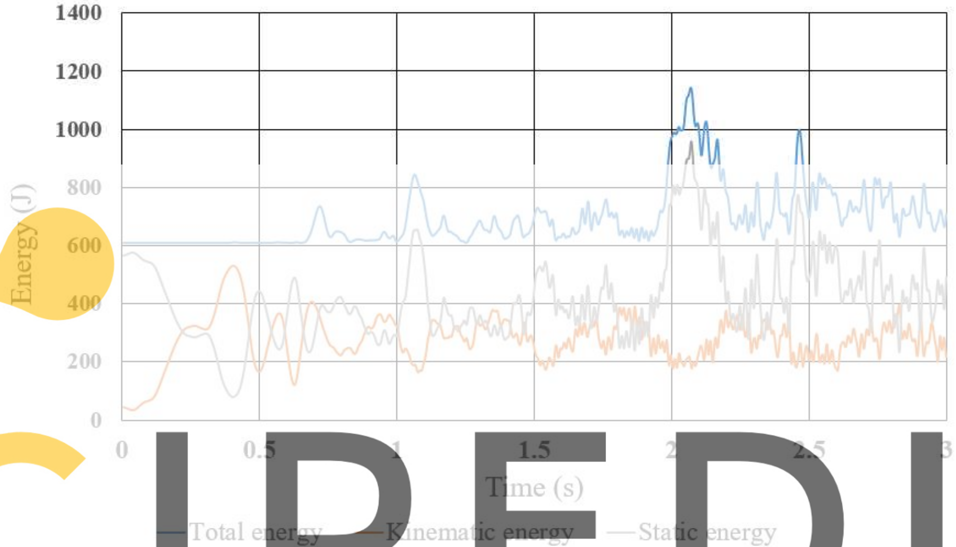

Figure 3: Energy distribution by free vibration

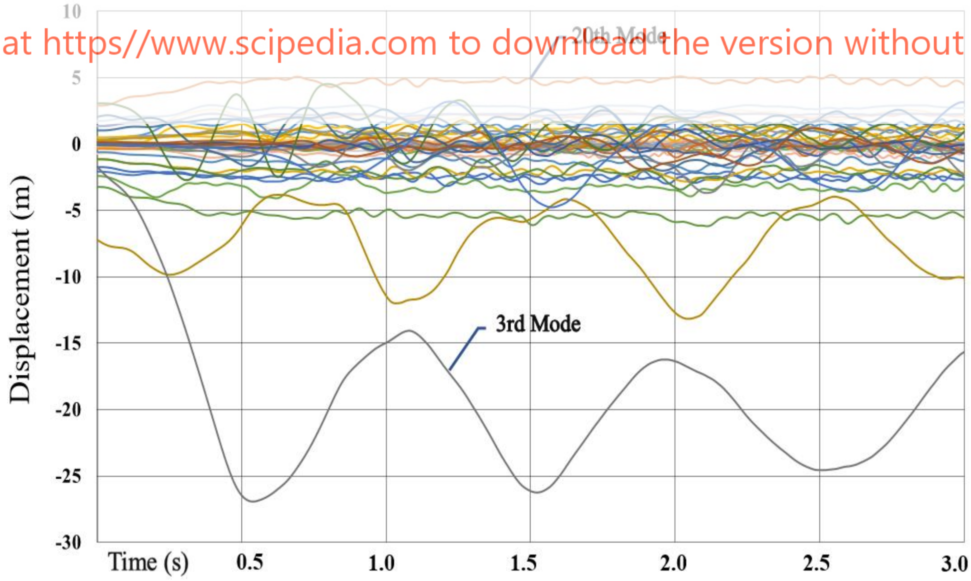

Figure 4: Result of mode decomposition

Table 2: Result of Eigen value analysis

Mode	Eigenvalue	Mode	Eigenvalue	Mode	Eigenvalue	Mode	Eigenvalue
1	1.24E+01	14	1.97E+03	27	1.17E+04	40	5.17E+04
2	1.26E+01	15	1.99E+03	28	1.22E+04	41	5.23E+04
3	1.82E+01	16	2.14E+03	29	1.31E+04	42	5.25E+04
4	5.08E+01	17	2.79E+03	30	1.52E+04	43	8.20E+08
5	1.22E+02	18	4.13E+03	31	1.85E+04	44	8.37E+08
6	1.61E+02	19	4.81E+03	32	1.99E+04	45	1.50E+09
7	2.10E+02	20	5.32E+03	33	2.06E+04	46	1.50E+09
8	2.15E+02	21	6.44E+03	34	2.27E+04	47	1.50E+09
9	3.26E+02	22	6.55E+03	35	2.32E+04	48	1.68E+09
10	5.40E+02	23	6.62E+03	36	3.72E+04	49	1.68E+09
11	6.86E+02	24	7.85E+03	37	4.01E+04	50	1.68E+09
12	1.00E+03	25	8.88E+03	38	4.94E+04	51	1.68E+09
13	1.60E+03	26	1.00E+04	39	5.06E+04	52	1.68E+09

5 FOLDING PROCESS BY COMPULSORY DISPLACEMENT

The equilibrium solution of figure 2(b) is taken as a base model for the folding process. And, all the free nodes (green color) in the middle and top layer of tensegrity model is given as constrained points (yellow color) as in figure 5.

(a) Before giving constraints (b) After giving constraints

Figure 5: Assignment of constrained nodes

The height of equilibrium model is checked and the number of steps for folding is designated to determine the appropriate displacement to be given. The lowest nodes are the base points so that no compulsory displacement is needed. For the topmost nodes, the full amount of compulsory displacement is given and for the layer-connecting middle nodes, half amount of designated displacement is enough to proceed the folding process. In this way, the process of folding the tensegrity model is successfully achieved in all cases of strut and cable material combination without the requirement of any complicated calculation. The resulted solution is a perfectly folded two-dimensional equilibrium configuration. The figure 6 to figure 8 show the illustration of (a) bird's eye view and (b) side view of folding model gradually at step 3, step 7 and the final step 10.

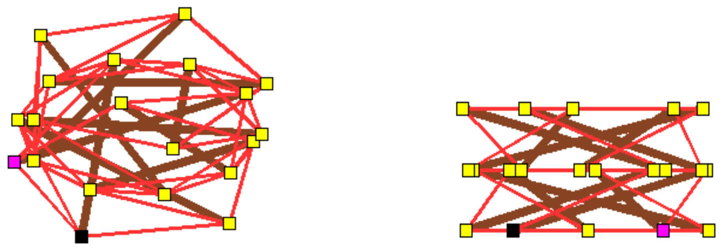

(a) Before giving constraints (b) After giving constraints

Figure 6: Folding tensegrity model at step 3

(a) Before giving constraints (b) After giving constraints

Figure 7: Folding tensegrity model at step 7

(a) Before giving constraints (b) After giving constraints

Figure 8: Folding tensegrity model at step 10

6 DEPLOYMENT BY DYNAMIC APPROACH

After the folding process of tensegrity by the compulsory displacement, the given constrained nodes will be released as in figure 9. Deploying into its original self-equilibrium configuration will be established by the performance of dynamic approach. In this time, the damping effect will be taken into account in which the value of Rayleigh coefficients and other required dynamic data are specified as shown in table 3.

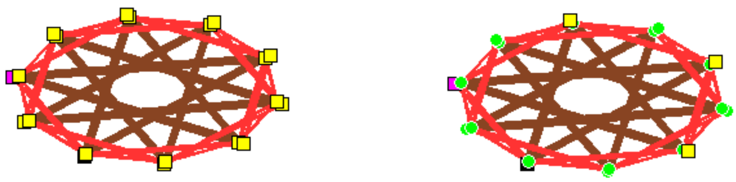

(b) Before giving constraints (b) After giving constraints

Figure 9: Assignment of constrained nodes

Table 3: Specification of dynamic data

Member	Strut	Cable
Material	Aluminum	Rubber
Specific gravity	2.7	1
Damping coefficients	Attenuation to mass α=1.612	Attenuation to stiffness β=0.0052
Time Specification	Time increment Δt=0.001 sec	Time limitation t=8 sec

6.1 Procedure of dynamic analysis

In the final part of our consistent algorithm, the deployment of folded tensegrity will be performed by dynamic analysis. Figure 10 demonstrates the general flow of dynamic procedure adopted in this study. The specified launch load is applied to all the free nodes of middle and top layer of folded tensegrity in order to initiate the vibration. In this process, the free nodes of tensegrity model will undergo the oscillatory mechanism in which the multi-degree-of-freedom will be realized in this system.

Since the deployment process of our proposed tensegrity will be implemented by the dynamic analysis involving large displacement, the performance of the nonlinear dynamic calculations is based on time integration method. This method time integration method evaluates the dynamic response of a structure under a given loading that may vary over a specified time function. Time integration method is a behavioral study of a structure in which the amplitude or acceleration of the structure is calculated for each time increment. This practice may require more calculation time, but produce the precise and accurate results.

Let the acceleration, velocity and displacement under the loading of P_i at the current time t_i as $\ddot{u}_i$, $\dot{u}_i$ and u_i respectively which are "known values", then equation of motion at current state can be rewritten in the scalar form as follow.

$$m\ddot{u}_i + c\,\dot{u}_i + ku_i = P_i \tag{17}$$

The change in structural response after the time increment Δt can be expressed as follow.

$$m\ddot{u}_{i+1} + c\,\dot{u}_{i+1} + ku_{i+1} = P_{i+1} \tag{18}$$

The "unknown values" of mechanical values at consecutive time step t_{i+1} can be obtained by several numerical methods. In this study, Newmark β method is adopted which is one of the most efficient methods in the time integration algorithm. This implicit method calculates the mechanical quantities of next time step based on the current condition and the resulted solutions will be renewed into the consecutive step. This iteration process will be repeated over the specified time function and terminated when the time increment reaches the limited time interval, and output the mechanical quantities.

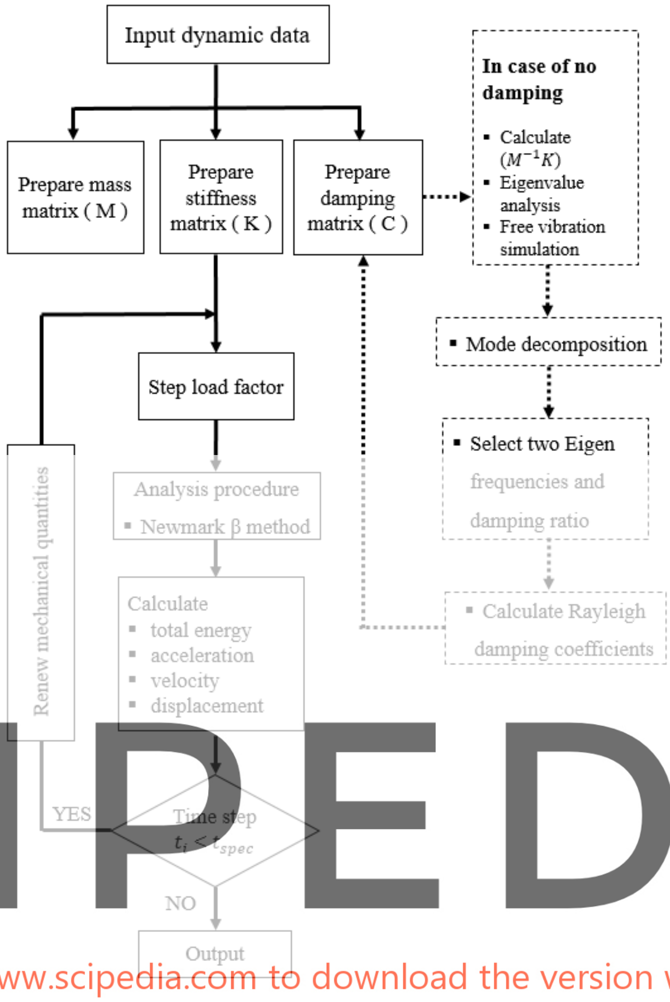

Figure 10: Flow chart of dynamic procedure

6.2 Stages of deploying tensegrity model

Figure 11 is the illustration of deployment process of proposed tensegrity model. The model is in a large deformation and tends to retain its original configuration within the first 3 seconds. After the oscillatory mechanism is gradually slow down due to the damping effect, the stably full scale deployment is achieved within the specified time limit of 8 seconds. The grey color in the models indicates the compression strain where relaxation occurs in cable condition.

Figure 12 and figure 13 show the displacement of one top node of proposed model, and the energy distribution of the whole structure, respectively. From these graphs, it can be seen that the structure oscillates greatly with high amount of energy within the first 3 seconds of deployment process. However, the treatment of proper damping makes the structure gradually stable and the kinematic energy is getting closer to zero within 3~6 seconds and keeps its stability until the specified time limitation. In this way, the folded tensegrity model makes its full deployment entirely and the simulation of dynamic analysis is successfully accomplished by selecting appropriate mode displacement and corresponding damping coefficient.

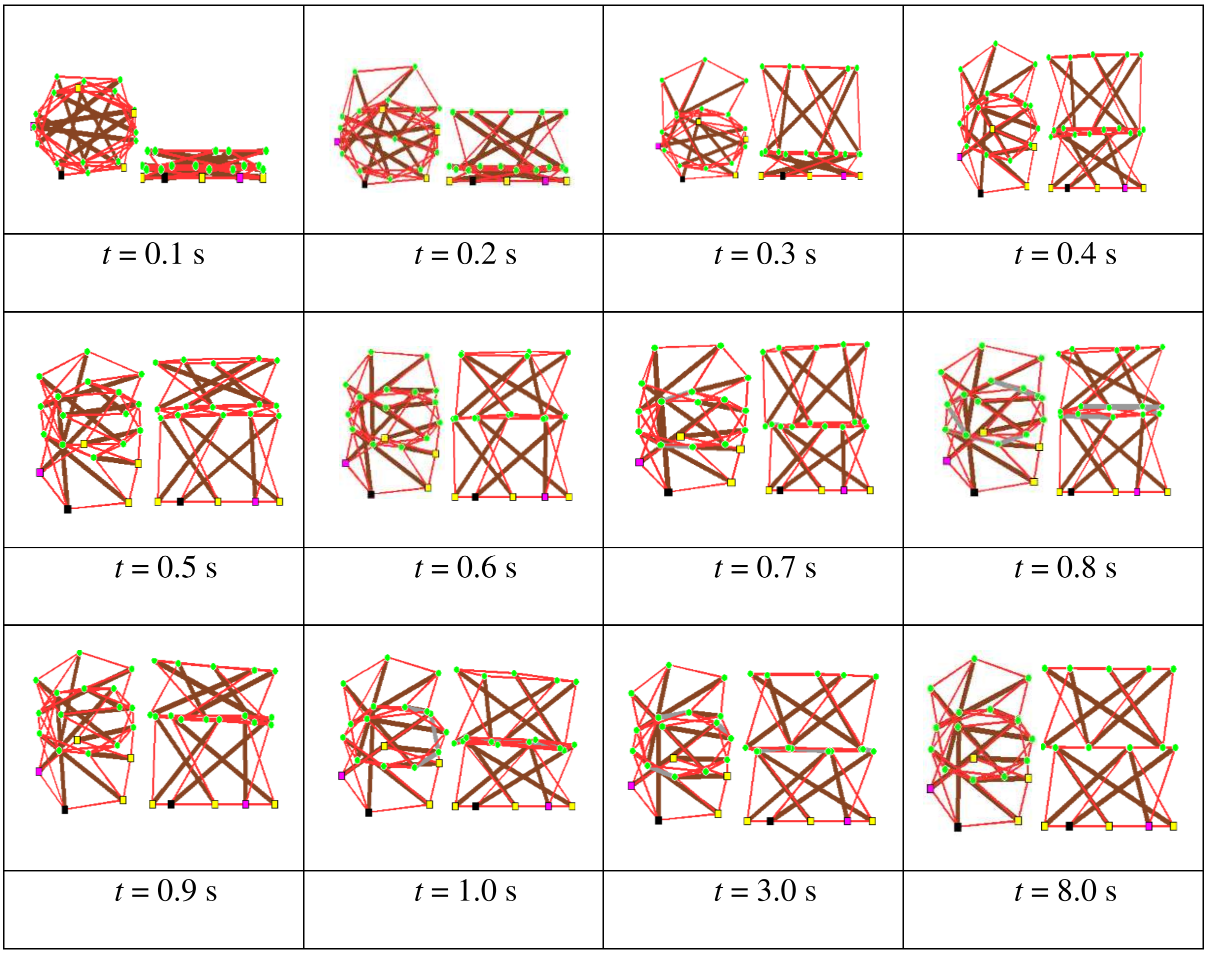

Figure 11: Stages of tensegrity deployment

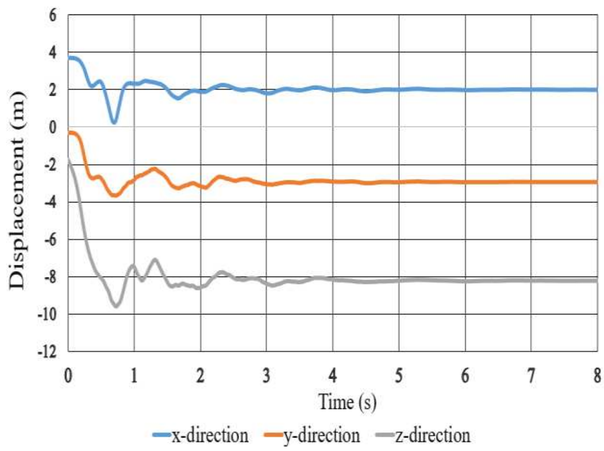

Figure 12: Displacement of top node

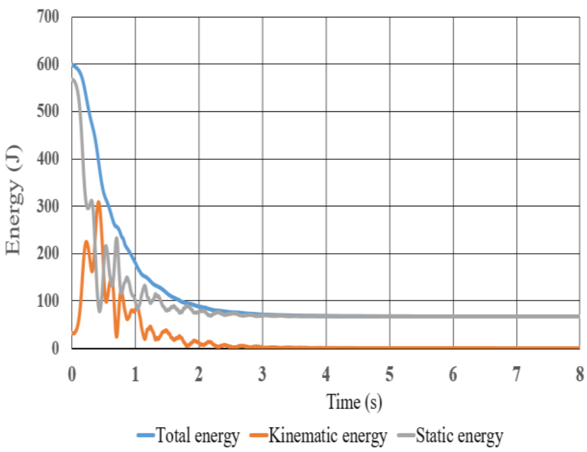

Figure 13: Energy distribution under damping effect

7 CONCLUSION

In this study, a simple tensegrity structure is proposed as a numerical model to conduct a series of structural analyses. In our consistent algorithm, form-finding analysis produces the equilibrium configuration by means of element's measure potential, and each member of the model is transformed into real element. The combination of aluminum struts and rubber cables makes the lightweight structure and the hyper-elastic material allows the tensegrity model to perform large deformation analysis. Static folding of tensegrity is simply achieved by the application of compulsory displacement, producing a perfectly folded tensegrity without the need of complicated calculation process. The deployment process is simulated by the dynamic analysis, considering damping effect. The mode decomposition by the Eigen value analysis helps to determine the appropriate amount of damping coefficients. In this way, the oscillatory mechanism is successfully achieved and kinematic energy is gradually reduced which makes tensegrity model to perform a stable full-scale deployment. Therefore, the proposed algorithm gives a reliable solution for both static and dynamic problems in geometrical nonlinear analysis.

REFERENCES

[1] A. Matsuo, H. Obiya, K. Ijima and M. Zakaria, "Form-finding of extensive tensegrity using truss elements and axial force lines," in *Int. Conf. on Textie Compsites and Inflatable Structures, Structural Membrane 2011*, October 2011.

[2] S. Ali and R. Motro, "FOLDABLE / UNFOLDABLE CURVED TENSEGRITY SYSTEMS," *JOURNAL OF THE INTERNATIONAL ASSOCIATION FOR SHELL AND SPATIAL STRUCTURES: J. IASS,* vol. 48, no. 3, pp. 153-160, December 2007.

[3] N. Ali and I. Smith, "Dynamic behavior and vibration control of a tensegrity structure," *International Journal of Solids and Structures,* vol. 47, no. 9, p. 12851296, 2010.

[4] Z. Kan, H. Peng, B. Chen and W. Zhong, "Nonlinear dynamic and deployment analysis of clustered tensegrity structures using a positional formulation FEM," *Composite Structures,* vol. 187, pp. 241-258, March 2018.

[5] J.Pinaud, Soren Solari, R. Skelton , "Deployment of a class 2 tensegrity boom," *Proceedings of the SPIE,* vol. 5390, pp. 155-162, July 2004.

[6] Cornel Sultan and Robert Skelton , "Deployment of tensegrity structures," *International Journal of Solids and Structures ,* vol. 40, no. 18, pp. 4637-4657, September 2003.

[7] M. Masic and R. Skelton, "Selection of prestress for optimal dynamic/control performance of tensegrity structures," *International Journal of Solids and Structures,* vol. 43, no. 7-8, pp. 2110-2125, 2006.

[8] Chan W, Arbelaez D, Bossens F, Skleton R.E, "Active vibration control of a three-stage tensegrity structure," in *In: SPIE 11th Annual International Symposium on Smart Structures and Materials*, San Diego, California, USA., 2004.